

# Wet snow-cover mapping by C- and L-band polarimetric SAR

Marit Holden, Anne Schistad Solberg and Rune Solberg  
Norwegian Computing Center, P.O. Box 114 Blindern, N-0314 Oslo, NORWAY  
Phone: +47 22 85 25 00 Fax: +47 22 69 76 60  
e-mail: Marit.Holden@nr.no Anne.Solberg@nr.no Rune.Solberg@nr.no

## Abstract

The main focus of this paper is discrimination between snow and bare ground for snow cover mapping using airborne EMISAR multipolarization SAR data. A series of three experiments investigating (i) the effect of the local incidence angle; (ii) the optimal subset of polarimetric features for best accuracy; and (iii) the optimal classifier was performed.

The backscatter values vary with local incidence angle. When this was corrected the backscatter values were less dependent on the incidence angle. Nevertheless, the classification accuracy was not significantly better using angle-corrected data in comparison to non-corrected data.

A number of studies have proposed and compared different features derived from multipolarization measurements. The aim of the second experiment was to find an optimal subset of such features. The highest classification accuracies were obtained for a one-dimensional feature vector consisting of C-band span, VH, or HV polarization.

Several supervised and unsupervised classification methods were studied. It turned out that, for this data set, clustering gave as good results as the supervised classifiers and the more complicated unsupervised classifiers studied.

## INTRODUCTION

The European Multi-sensor Airborne Campaign (EMAC '94/95) program for 1995 included snow and ice experiments in northern Europe. The aim was to test new sensors for improved quality of snow and ice measurements. The snow and ice test sites are found in northern Finland, in the gulf of Bothnia (Finland), and in northern Norway. The data analyzed in the experiments described in this paper are from the test site in northern Norway, which is located at Kongsfjellet near the Okstindan glacier (66° N, 14° E).

This paper describes a series of three experiments investigating the effect of the local incidence angle, the optimal subset of polarimetric features, and the optimal classification algorithm for snow-cover mapping.

The backscattering signal for snow and bare ground

varies with the local incidence angle. We will illustrate that this is the case for the data studied here. Then, we will correct the backscattering signal to reduce this variation and perform experiments to find out how this influences the classification accuracy.

Many features for use in classification may be derived from the polarimetric SAR data. To find an optimal subset of such features an automatic feature selection method will be used. This is done to indicate the optimal near-future SAR satellite sensor for snow-cover mapping.

In the last experiment, we will study two supervised and three unsupervised classifiers. For operational applications, unsupervised classifiers are the most useful. Therefore, it is interesting to compare the behavior of such classifiers to that of the supervised ones.

## THE DATA SET

The available data set consists of airborne EMISAR C- and L-band polarimetric SAR data. Three data sets, from March, May, and July 1995, were acquired. In the experiments described in this paper only the July data set has been investigated.

A comprehensive field work was carried out simultaneously with the SAR acquisitions. Nine snow parameters were measured: Density, liquid water content, water equivalent, snowpack structure, temperature, snow depth, snow grain size, snow surface roughness, and snow coverage. For the July campaign, the area was covered by aerial infrared photography in order to determine the exact snow cover and the vegetation type in bare-ground areas. An orthophoto was derived from the aerial photos.

The SAR data were geocoded by NORUT IT. The images were first geometrically corrected, then transformed to UTM coordinates. In this process a digital elevation model was used. This model was also used for finding the local incidence angle of each pixel. Before classifying these data, they were mean filtered using a  $3 \times 3$  window. The original SAR data had a resolution of  $1.5 \text{ m} \times 1.83 \text{ m}$ . During the geocoding process they were resampled to pixel size  $5 \text{ m} \times 5 \text{ m}$ .

The orthophoto had a resolution of  $1 \text{ m} \times 1 \text{ m}$ . To get

the same resolution as the SAR data it was resampled to pixel size  $5\text{ m} \times 5\text{ m}$ , using nearest neighbor resampling.

## METHODS AND RESULTS

**Ground truth** Three main classes were present in the July data set: wet snow, bare ground (e.g. mountain birch), and sparse vegetation (e.g. bed rock, moss, heather). Ground truth was obtained from the orthophoto by thresholding in order to divide the data set into snow and not-snow pixels. The result of this was modified manually because the thresholding did not give a perfect result in areas with shadow. The not-snow pixels were further separated into bare ground and sparse vegetation using a digital map of the area. The digital map was also used to identify and remove lakes from the data set.

**The effect of local incidence angle** The backscattering signal for snow and bare ground varies with the local incidence angle. This is expected to influence the classification performance. Various models for correcting the angle dependency have been reported, the most common correction is to apply a correction factor involving the *cosine* of the incidence angle (e.g. see [5]).

In the uppermost part of Figure 1 this dependency is illustrated for snow, bare ground, and sparse vegetation in the very rough terrain of the test site. The mean backscatter value for all pixels corresponding to a certain incidence angle is plotted for each of the three classes. We observe that the backscatter value is higher for larger angles. Only C-band HV-polarization results are shown in the illustrations. Similar result were obtained also for the other C-band polarizations.

For reducing the backscatter values dependency of angle Shi and Dozier [5] multiply the backscatter values by  $\cos^a(\alpha)$ . Here  $a$  is some positive constant and  $\alpha$  is the local incidence angle, or more precisely the angle between the local surface normal and the image plane normal.

In the two middle illustrations of Figure 1, we see the results of correcting the backscatter values for  $a = 1, 2$ . We observe that the corrections lead to a small angle dependency for angles below 60-80 degrees. For the extreme angles, on the other hand, the result is not satisfactory. To avoid this undesirable effect we corrected the backscatter signal by multiplying by  $\cos^a(\alpha)$  for angles below 60 degrees and with  $\cos^a(60)$  for angles above 60 degrees. In the lower part of Figure 1, we see the result of performing this correction with  $a = 2$ . We observe that we now avoid the effect with bad results for extreme angles, and that the backscatter values vary less with angle than they did without angle correction.

Let us next study how the angle correction of the backscatter signal influences the classification accuracy. The classification method used is K-means clustering [1]. We clustered the data into five clusters and let two of the clusters be snow and the three others be snow free. Initial

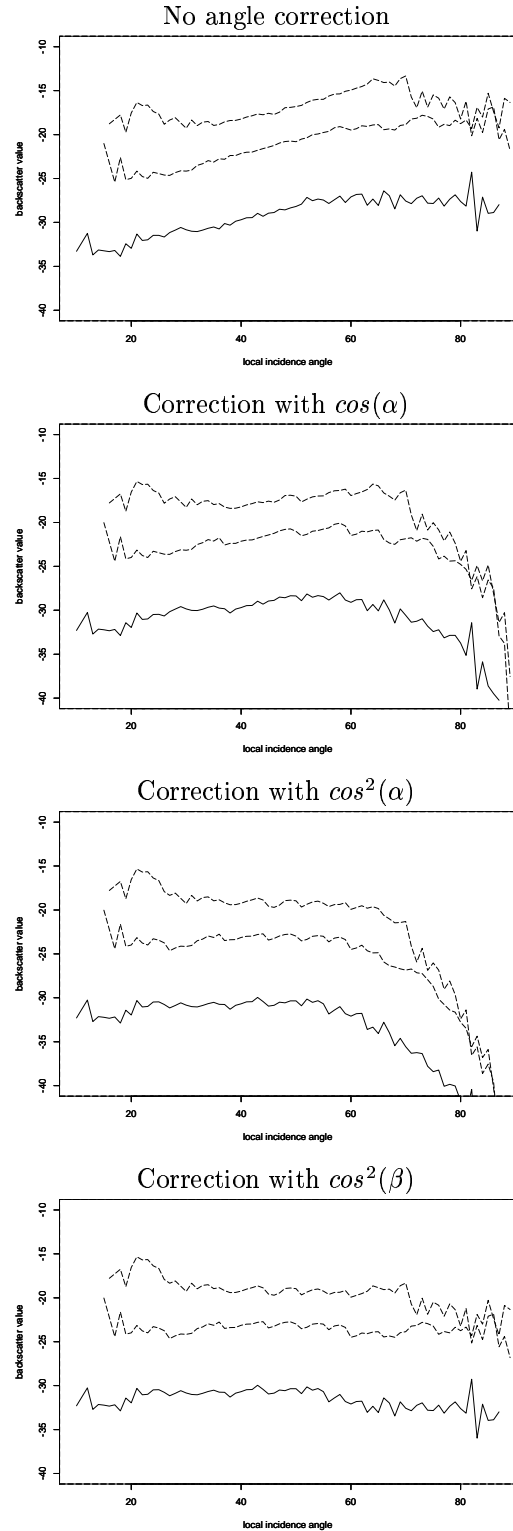


Figure 1: Plots of the  $\sigma_{0dB}^2$ -backscatter C-band HV value compared to local incidence angle for snow (lower curve), bare ground (middle curve) and vegetation (upper curve).  $\alpha$  is the incidence angle.  $\beta$  is equal to  $\alpha$  when  $\alpha < 60^\circ$  and  $60^\circ$  otherwise.

Polarization	HH	HV	VH	VV
No correction	84.4	85.0	85.3	84.0
$\cos^1(\alpha)$	85.1	85.2	85.5	84.8
$\cos^2(\alpha)$	85.2	85.4	85.1	84.4
$\cos^2(\beta)$	85.5	85.7	85.4	84.6

Table 1: *Classification accuracies when clustering the C-band data into five clusters to separate snow from snow free.  $\alpha$  is the incidence angle.  $\beta$  is equal to  $\alpha$  when  $\alpha < 60^\circ$  and  $60^\circ$  otherwise.*

seed values near the mean of the snow class were used for the two snow clusters. For the three snow free clusters values near and between the means of the two other classes were used. Let  $\alpha$  be the incidence angle. Let  $\beta$  be equal to  $\alpha$  when  $\alpha < 60^\circ$  and  $60^\circ$  otherwise. For each C-band polarization we performed four clusterings, one for the uncorrected data, one for data corrected with  $\cos(\alpha)$ , one with  $\cos^2(\alpha)$ , and one with  $\cos^2(\beta)$ . In Table 1 the classification accuracy for each case is given. We observe that the classification accuracies are only slightly influenced by the angle correction. We would perhaps have expected improved classification accuracy after angle correction, especially for the correction factor  $\cos^2(\beta)$ . A reason for obtaining only small improvements might be that the snow and snow free classes already are quite well separated (see Figure 1).

**Optimal subset of polarization features** In the event of a polarimetric satellite SAR, this second experiment studies the classification performance for subsets of single polarization and dual polarization features compared to full polarimetric data. A number of studies have proposed and compared different features derived from multipolarization measurements. It is expected that polarization features which involve the ratio between two polarizations or frequencies are more robust with respect to the incidence angle effect than features based on a single polarization [3, 5].

The set of features considered consists of 20 features found in the literature. The set contains for both C- and L-band the four polarizations (HH, HV, VH, VV), the span ( $\frac{HH+HV+VH+VV}{4}$ ) [4], the depolarization factors (HV/VV, VH/HH) [7], and the copolarization ratio (HH/VV) [4]. In addition we included for each polarization the feature: L-band polarization divided by C-band polarization [4]. The depolarization ratio is expected to discriminate between areas with multiple scatterers (e.g. rock) and smoother surfaces (e.g. snow). The copolarization ratio  $HH/VV$  is expected to be smaller for wet snow than for rough surfaces [5].

To choose an optimal subset from these 20 features an automatic feature selection method was used. This method was based on an iterative inclusion of the best features [6]. For computing error rates the leave-one-out

Snow separated from bare ground

Feature	
C-band span	87.2%
C-band VV	84.1%
C-band HH	83.9%
all other features	79.0% or worse

Snow separated from vegetation

Features	
C-band HV	95.1%
C-band VH	95.0%
L-band HV	94.2%
L-band VH	94.2%
C-band span	91.0%
all other features	88.8% or worse

Table 2: *Classification accuracies obtained in the two automatic feature selection experiments.*

method and a Gaussian maximum likelihood classifier was used.

We performed two experiments with the automatic feature selection method. First we chose a set of features for separating snow from bare ground. Then we chose a set of features for separating snow from vegetation. Both these experiments indicated that a set containing several features is only slightly better than a set consisting of only one feature. The classification accuracies obtained in the two experiments are summarized in table 2.

To find a set of features which separates snow from both bare ground and vegetation we investigated further the following features: C-band HV and VH, C-band span, and L-band HV and VH. These features were chosen because C-band span was clearly best in the snow/bare ground experiment, and because the four others were the only features with better results in the snow/vegetation experiment (see table 2). To find the best of these five features, we clustered the data using K-means clustering as above. The classification accuracies are given in table 3. As expected, the results for C-band HV and VH are almost the same because these two polarizations contain more or less the same information. Similarly for L-band HV and VH. To find out whether a set consisting of more than one feature leads to better results than a set consisting of only one feature, we found the classification accuracy for subsets consisting of two or three of C-band HV, C-band span, and L-band HV. As we see from table 3 the results are not improved when several features were used. Concerning the result for one-dimensional feature vectors, the best results were obtained for C-band HV, VH and span. Near future sensors will normally not be fully polarimetric. Since span involves all the four polarizations we conclude that C-band VH or HV polarization is the optimal feature to use for snow discrimination on data sets similar to the one in the present study.

Features	
C-band HV	85.6%
C-band VH	85.5%
C-band span	85.7%
L-band HV	76.8%
L-band VH	76.7%
C-band HV + L-band HV	83.9%
C-band HV + C-band span	85.6%
L-band HV + C-band span	83.7%
C-band HV + L-band HV + C-band span	84.9%

Table 3: *Classification accuracies obtained when clustering the data into five clusters to separate snow from snow free. The data set clustered is equal to the test set described in the paragraph concerning the optimal classifiers.*

In Shi and Dozier [5] the depolarization and copolarization factors gave good results. However, their reported average performance compared to intensity measurements seems to involve classes of different sizes, and by considering the number of pixels in each class in computing the average performance, the difference between using only C-band VV compared to multipolarization measurements is not very large. For our data set, we obtain the following accuracies for these features: C-band HH/VV 51.3%, C-band HV/VV 67.7%, and C-band VH/HH 63.2%. This indicates that some discriminatory power present in the absolute value of the calibrated polarization measurements is lost by computing normalized features involving two measurements.

**Optimal classifier** In this last experiment, we will classify the data set using both supervised and unsupervised classifiers. The data set was separated into a training set and a test set. The classification accuracies given are for this test set. The feature used in the following experiments is C-band span, which was one of the three best features found in the experiment above.

Two supervised classifiers were applied. These are a noncontextual and a contextual Gaussian maximum likelihood classifier. The contextual classifier used is the Haslett classifier (see [2]). For these two classification methods we obtained the following accuracies: non-contextual classification 85.4% and contextual classification 85.7%. The non-contextual classification result for a part of the data set is found in Figure 2.

Besides K-means clustering, which gave an accuracy of 85.7%, two other unsupervised classifiers were used. These are combinations of clustering and one of the two supervised classifiers mentioned above. Here, clustering is first done to be able to perform automatic training. Then the result is used to train the two (non-contextual and contextual) Gaussian maximum likelihood classifiers. For these two classification methods we obtained the following accuracies: clustering combined with non-contextual classi-

fication 85.6% and clustering combined with contextual classification 85.9%.

We observe that the classification accuracies obtained above are very similar. Since unsupervised classifiers are most useful for operational applications, such a classifier will be preferred. Clustering is as good as any of the other unsupervised classification techniques. We therefore conclude that this is the best for the data set studied here.

The clustering scheme described above is not totally unsupervised because the seeds are chosen with respect to the mean values of the three classes. On the other hand, it should be possible to automatically choose reasonable values for the seeds because the approximate mean backscatter values of the classes present in the scene are known in advance. By using these values combined with histogram information it should be possible to choose seeds points not too far from those we chose manually here. Nevertheless, it should be further investigated how dependent the clustering results are on the initial seed points.

## CONCLUSION

In the first experiment of this paper, the effect of the local incidence angle on the backscattering signal was investigated. We observed that the backscatter values varied with local incidence angle and corrected them so that this variation became less. This correction did not significantly improve the classification accuracy.

In the next experiment an optimal subset of features derived from multipolarization measurements was selected. We concluded that a subset consisting of one of the C-band copolarizations (HV or VH) or span was the optimal one.

Several supervised and unsupervised classification methods were studied. It turned out that, for this data set, clustering gave as good results as the supervised classifiers and the more complicated unsupervised classifiers studied. It should be further investigated how dependent the clustering result is of the initial seed points, which were manually picked out in the present study.

**Acknowledgment** This work is carried out within SNOW-TOOLS, an Environment and Climate project funded by Commission of the European Community, Contract no. ENV4-CT96-0304. We would also like to thank NORUT IT for geocoding the SAR data.

## References

- [1] R. O. Duda and P. E. Hart. *Pattern Classification and Scene Analysis*. John Wiley & Sons, New York, 1973.
- [2] J. Haslett. Maximum Likelihood Discriminant Analysis on the Plane Using a Markovian Model of Spatial Context. *Pattern Recognition*, 18:287–296, 1985.

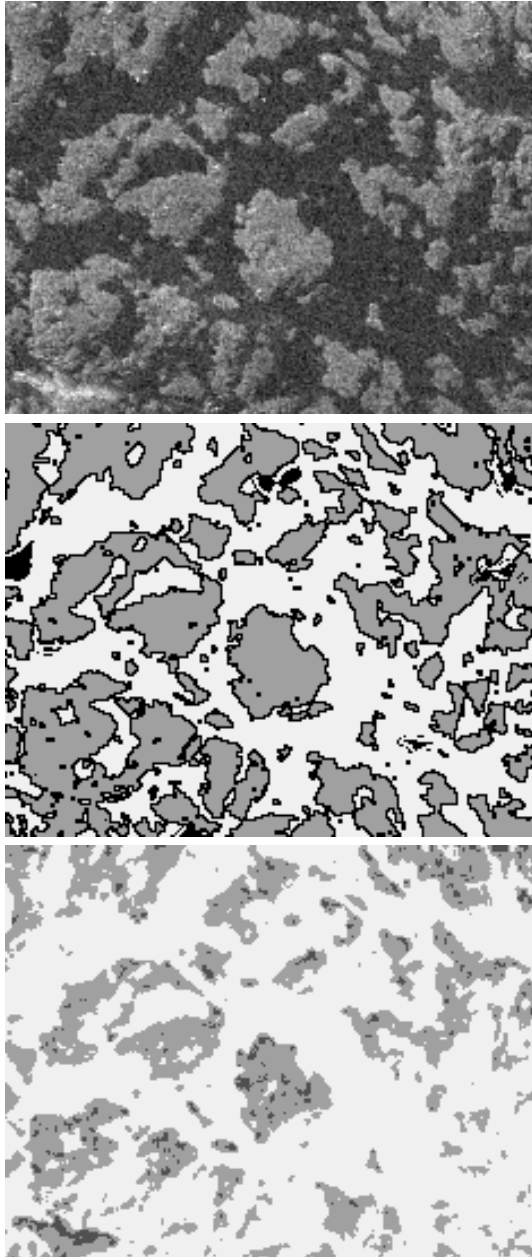


Figure 2: *Upper image: Part of the C-band VH-polarization data. Middle image: The corresponding ground truth image - snow is white, bare ground is grey, and pixels not belonging to any class are black. Lower image: The result of non-contextual classification - snow is white, bare ground is light grey, and sparse vegetation is dark grey. When the classification accuracy was computed, only pixels for which we have ground truth were used.*

- [3] H. Rott and R. E. Davies. Multifrequency and polarimetric SAR observations on alpine glaciers. *Annals of Glaciology*, 17:98–104, 1993.
- [4] J. Shi and J. Dozier. Mapping Seasonal Snow with SIR-C/X-SAR in Mountainous Areas. *Remote Sensing of Environment*, 59:294–307, 1997.
- [5] J. Shi, J. Dozier, and H. Rott. Snow Mapping in Alpine Regions with Synthetic Aperture Radar. *IEEE Transactions on Geoscience and Remote Sensing*, 32(1):152–158, 1994.
- [6] R. Solberg and T. Egeland. Automatic feature selection in hyperspectral satellite imager. In *IGARSS'93*, 1993.
- [7] F. T. Ulaby, R.K. Moore, and A. K. Fung. *Microwave Remote Sensing: From Theory to Applications*, volume III. Addison-Wesley Publishing Company, Inc, Reading, Massachusetts, 1986.